Chemical Oxidation of the Ligand in Nickel(II) Cyclam: Formation of a Novel Dinuclear Complex and of a Related Cation Containing a Ligand Radical Ion

A. McAuley* and C. Xu

Chemistry Department, University of Victoria, Victoria, BC V8W 3P6, Canada

Received May 12, 1992

Reaction of nickel(II) cyclam (cyclam = 1,4,8,11-tetraazacyclotetradecane) with hydrogen peroxide in acidic perchlorate media results in the formation of a dimeric complex $[Ni_2(1,1'$-enebicyclo-3,6,10,13-tetraazatetradeca-2,13-dienylidene))$](ClO_4)_4$, $[Ni_2(L4)](ClO_4)_4$, in which there is evidence for electron delocalization across the M–M distance. The dinuclear complex crystallizes in the triclinic space group $P\bar{1}$ (No. 2). Refinement of the structure for $[Ni_2(L4)](ClO_4)_4$ (a = 8.557 (1), b = 13.382 (2), c = 8.475 (2) Å; α = 107.45 (2), β = 116.62 (2), γ = 76.21 (1)°; Z = 2 molecules) converged at R = 0.0665 (R_w = 0.0654) for 226 parameters, using 1404 reflections with $I > 2\sigma(I)$. The entire complex ion consists of a series of planes which imparts an "S"-shaped form to the structure. Within each macrocycle, the nickel is situated in the plane of the four nitrogen donors and there is planarity across the carbon bridging framework. The imine distances (1.296 (13) Å) are longer than those characteristic of that group. Chemical or electrochemical reduction results in the formation of a radical ion (VI), which exhibits an intense absorption at 724 nm ($\epsilon = 1.4 \times 10^4$ M^{-1} cm^{-1}) and an ESR spectrum centered close to the free electron but broadened probably owing to the presence of the metal ions in the ion. This species is stable in the absence of air but is readily reoxidized to the parent ion. A mechanism is proposed for the formation of the dimeric species. Preliminary data on the rate of reduction by $[Co(phen)_3]^{2+}$ are presented.

Introduction

Investigations into the redox and protonation chemistry of diimine species derived from the reaction of coordinated amines with β-diketones[1-10] have been well documented. In some instances, the metal and ligand orbitals are comparable in energy such that a metal–ligand molecular orbital (MLMO) is formed which is the center of chemical activity. One of the earliest reports on such a system involves (11,13-dimethyl-1,4,7,10-tetraazacyclotrideca-10,12-dienato)nickel(II) perchlorate, $[Ni(AT)]ClO_4$ (**1**).[3,6] This complex displays significant aromaticity on its six-membered dienato(–) ring.[5] Subsequently, redox reactions of $[Ni(AT)]^+$ and the corresponding 14-membered ring analog $[Ni(Me_2[14]\text{-}4,7\text{-}[14]\text{-dieno}(-)N_4)]^+$, $[Ni(AT')]^+$ (**2**) were investigated.[4] Oxidation of the complexes containing diimine moieties takes place relatively easily[7,8] and is more or less independent of the metal center involved.

More recently, quasi-aromatic molecular structures of (2,2,3,9,-10,10-hexamethyl-5,7-dioxa-6-hydra-1,4,8,11-tetraazacyclotetradeca-3,8,11,13-tetraene)nickel(II), $[Ni(PnAO\text{–}6H)]^0$ (**3**), and its derivatives were described.[9] Internal electron transfer from the ligand to the metal center has also been reported[2,8] for M(III) complexes (M = Co, Ni) with a β-diiminato type ligand, e.g., $[Co(AT')(NCS)_2]^0$, where Co(III) oxidized the β-diiminato chelate to form a ligand radical species which subsequently dimerized to give a binuclear complex. The latter ion may be further dehydrogenated under mild conditions to yield an extended unsaturated bimetallic system. Direct coupling of two molecules

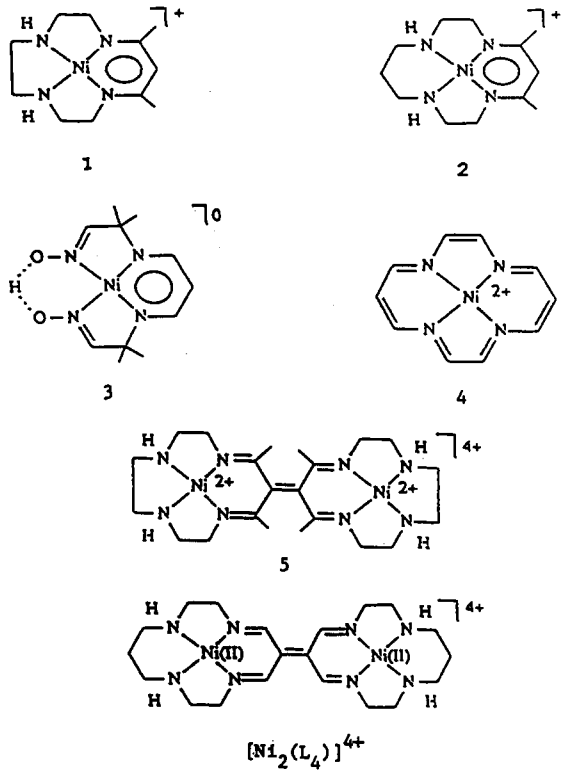

of **1** has also been reported.[11] Oxidation of the Ni(II) complex containing a highly conjugated [14]aneN$_4$ ligand (**4**) is predominantly ligand-based.[10] Chemical and electrochemical oxidation of a nickel(II) tetraazaannulene complex results in the formation of a binuclear nickel(II) species with the attainment of an aromatic structure.[13]

In the present study, we provide evidence for a unique multielectron oxidation of $[Ni^{II}cyclam]^{2+}$ (cyclam = 1,4,8,11-

(1) Melson, G. A., Ed. *Coordination Chemistry of Macrocyclic Compounds*; Plenum Press: New York, 1979.
(2) Lindoy, L. F. *The Chemistry of Macrocyclic Ligand Complexes*; Cambridge University Press: Cambridge, U.K., 1989.
(3) Cummings, S. C.; Sievers, R. E. *J. Am. Chem. Soc.* **1970**, *92*, 215; *Inorg. Chem.* **1970**, *9*, 1131.
(4) Martin, J. G.; Wei, R. M. C.; Cummings, S. C. *Inorg. Chem.* **1972**, *11*, 475.
(5) Richardson, M. F.; Sievers, R. E. *J. Am. Chem. Soc.* **1972**, *94*, 4134.
(6) Elfring, W. H., Jr.; Rose, N. J. *Inorg. Chem.* **1975**, *14*, 2759.
(7) Switzer, J. A.; Endicott, J. E.; Khalifa, M. A.; Rotzinger, F. P.; Kumar, K. *J. Am. Chem. Soc.* **1983**, *105*, 56.
(8) Endicott, J. E.; Durham, B. Reference 1, p 433.
(9) Murmann, R. K.; Vassian, E. G. *Coord. Chem. Rev.* **1990**, *105*, 56.
(10) Millar, M.; Holm, R. H. *J. Am. Chem. Soc.* **1975**, *97*, 6052.
(11) Switzer, J. A.; Endicott, J. F. *J. Am. Chem. Soc.* **1980**, *102*, 1181.
(12) Cummingham, J. A.; Sievers, R. E. *J. Am. Chem. Soc.* **1973**, *95*, 7183.
(13) McElroy, F. C.; Dabrowiak, J. C. *J. Am. Chem. Soc.* **1976**, *98*, 7112. Ferrara, G. P.; Dabrowiak, J. C. *Inorg. Nucl. Chem. Lett.* **1978**, *14*, 223.

0020-1669/92/1331-5549$03.00/0

Table I. Crystallographic Data for [Ni_2(1,1′-enebicyclo-3,6,10,13-tetraazatetradeca-2,13-dienylidene)](ClO_4)$_4$, [Ni_2(L4)](ClO_4)$_4$

chem formula: $Ni_2C_{20}H_{32}O_{16}Cl_4$	V = 821.5 Å^3
fw: 899.7	Z = 2 molecules
space group: $P\bar{1}$ (No. 2)	ρ_{calc} = 1.818 g cm^{-3}
a = 8.557 (1) Å	ρ_{meas} = 1.807 g cm^{-3}
b = 13.382 (2) Å	μ = 14.72 cm^{-1}
c = 8.475 (2) Å	T = 22 ± 2 °C
α = 107.45 (2)°	λ = 0.710 69 Å
β = 116.62 (2)°	$R(F_o)$ = 0.0665
γ = 76.21 (1)°	R_w = 0.0654

tetraazacyclotetradecane) with probable initial formation of a Ni(III) complex. Oxidative dehydrogenation within the six-membered ring of the ligand and subsequent coupling yield a binucleating macrocycle where each nickel(II) ion is square planar and there is extensive interaction between the centers. While this paper was being prepared for publication, a report appeared of an iron(II) species of the same ligand, where the formation took place via aerobic oxidation of [Fe^{II}cyclam]$^{2+}$ in acetonitrile.[14]

Experimental Section

All materials were of reagent grade, except where otherwise indicated. Infrared spectra were obtained on KBr disks by using a Perkin-Elmer 283 grating spectrometer. ESR spectra were measured on a Varian E6S spectrometer or a Bruker ER200tt instrument with an IBM-PC attachment. Diphenylpicrylhydrazyl (dpph; g = 2.0037) was used as a reference standard. UV–visible spectra were run on either a Cary 17 or a Perkin-Elmer Lambda 4B dual-beam spectrophotometer. Elemental analyses were performed by Canadian Microanalytical Services, Vancouver, BC, Canada. Electrochemical measurements were made by using a Princeton Applied Research Model 273 potentiostat/galvanostat. In acetonitrile, (t-Bu)$_4$NClO$_4$ (0.1 M) was used as the supporting electrolyte and Ag/AgNO$_3$ (0.1 M AgNO$_3$) as the reference electrode. Acetonitrile was freshly distilled over calcium hydride under an inert atmosphere immediately before use, and all solutions were deaerated with Ar. The study in aqueous media was carried out at various acidities in principally nitrate solutions (H^+/Na^+,NO_3^-, I = 1.0 M) using Ag/AgCl (saturated KCl) as the reference electrode. Unless otherwise specified, the potentials used are referenced to $Fc^{+/0}$ in CH_3CN (0.40 V vs NHE) and Ag/AgCl (0.222 V vs NHE) in aqueous solution. In the presentation of the results, only potentials relative to NHE are provided.

[Ni_2(1,1′-enebicyclo-3,6,10,13-tetraazatetradeca-2,13-dienylidene)](ClO_4)$_4$, [Ni(L4)](ClO_4)$_4$. To a stirred solution of nickel(II) cyclam perchlorate (1.0 g) in 1.0 M $HClO_4$ (30 mL), preheated to 70 °C, was added 1 mL of 30% H_2O_2. After the solution had turned to a dark red color, it was placed immediately in an ice/water bath. Within 10 min, a dark reddish precipitate was formed. The product was isolated by filtration, washed with ethanol and then ether, and air-dried. Yield: 0.227 g (25%).

X-ray-quality crystals of [Ni_2(L4)](ClO_4)$_4$ were obtained by dissolving 30 mg of material in 1.5 mL of H_2O, followed by addition of 5 drops of concentrated $HClO_4$. After 10 min, any precipitate formed was filtered off, and the supernatant was kept still and allowed to evaporate very slowly for 10 days. This procedure was repeated until X-ray-quality crystals were formed. IR: C=N stretch, 1610 cm^{-1}; C=C stretch, 1410 cm^{-1}; ClO_4^-, 1100, 620 cm^{-1}. Anal. Calcd for [$Ni_2C_{20}H_{36}N_8Cl_4O_{16}$]: C, 26.57; H, 3.98; N, 12.40. Found: C, 26.40; H, 3.82; N, 12.08.

Caution! Transition metal perchlorates are known to be hazardous and must be treated with care, especially in the presence of organic solvents.

Crystallography. The experimental parameters for the complex are presented in Table I. Dark wine-red crystals were mounted in glass Lindemann tubes and the unit cell and space group determined by using Weissenberg and precession photography, after which the crystal (dimensions 0.7 × 0.15 × 0.01 mm) was transferred to a Nonius CAD 4 diffractometer.

The unit cell was refined by using 21 pairs of reflections in the 2θ range 22–39°. Intensity measurements were carried out at 22 ± 2° in the ω–2θ scan mode with Zr-filtered Mo radiation, λ = 0.710 69 Å. A total of 1987 reflections were measured, from which 1404 [$I > 2\sigma(I)$] were used after suppression. Three standard reflections preceded each batch of 50 measurements, with no decomposition observed during the collection. Solution of the phase problem was achieved with direct methods using SHELX76.[15] The atomic scattering factors were those included in the SHELX76 program together with the Ni f curve from ref 16. The EMPABS (Nonius) program was used for absorption corrections. Completion and refinement of the structure were carried out by difference electron density maps and least-squares techniques. All atoms were refined anisotropically except for the hydrogens. The refinement converged with a maximum shift/esd of 0.011 on the final cycle. A final difference map showed a maximum peak of 0.755 e Å^{-3}.

Results

The macrobicyclic complex was synthesized in a multielectron oxidation of the ligand in [Ni^{II}cyclam]$^{2+}$, followed by a dimerization. In the present system, there is evidence for electron delocalization across the M–M distance. Crystallographic parameters are consistent with only partially localized diimine and C=C centers and are directly comparable with the similar iron(II) complex ion reported recently.[14] The dinuclear nickel complex undergoes a ready 1-e reduction to yield a radical ion (VI) with an intense absorption band at 724 nm (ϵ = 1.3 × 10^4 M^{-1} cm^{-1}) attributable to a LMCT band. Associated with this species is an ESR spectrum centered at g close to the free-electron value but broadened by interaction with the nickel centers. Further reduction is adduced from electrochemical measurements, where there is evidence for two 1-e processes. Studies with [Co(phen)$_3$]$^{2+}$ as an outer sphere reductant provide evidence for a two-step process, the first of which involves formation of the radical ion.

Discussion

Previous studies of the oxidation of [Ni^{II}cyclam]$^{2+}$ by using such reagents as Co^{III}_{aq}[17] and peroxodisulfate[18] in aqueous media led to the formation of Ni(III) complex ions where the d^7 ion has been characterized by ESR spectroscopy.[18] In the present system, further reaction produces a unique dinuclear ion with an extensive delocalized π-system, similar to the species involving two Fe(II) centers.[14] Coupling of diimine complexes has been investigated previously by other workers.[11-13]

Molecular Structure. Crystallographic data are listed in Table I, and atomic coordinates and selected interatomic distances and bond angles are presented in Tables II and III, respectively. An ORTEP drawing of molecular structure is shown in Figure 1a.

The molecule has a center of symmetry at the midpoint of its bridge, C(2)–C(2′). As shown in Table III, the latter bond distance, 1.402 Å, is intermediate between those for a single C—C bond (1.50 Å) and a double C=C bond (1.34 Å). (For a more direct comparison, the single-bond bridge found in bis[nickel(II) cyclam] is 1.542 Å,[19] and the localized double-bond bridge in [Ni(ATH)]$_2^{4+}$ (**5**; vide infra) is 1.344 Å.[12]) This reflects some delocalization of electron density, which is also exhibited in the imine bonds in the six-membered rings. In this case, the average (1.297 (13) Å) is longer than that (1.26–1.27 Å) for π-electron-localized C=N bonds. These delocalization characteristics are reflected in lower energy shifts of C=N (1600 from 1650 cm^{-1}) and C=C (1410 from 1600 cm^{-1}) stretches in the IR spectrum. In addition, the carbon–carbon single bonds (C(1)—C(2) and C(2)—C(3)) on the diimine ring are shortened. On average, these are 0.074 Å shorter than the rest of the C—C bonds in the molecule (d_{av}(C—$C_{delocal}$) = 1.459 (16) Å vs d_{av}(C—C_{local}) = 1.533 Å). The C=C, C=N, and C—C distances are almost identical to those found recently in the iron(II) complex of the same ligand.

(14) Mountford, H. S.; Spreer, L. O.; Otvos, J. W.; Calvin, M.; Brewer, K. J.; Richter, M.; Scott, B. *Inorg. Chem.* **1992**, *31*, 718.

(15) Sheldrick, G. M. SHELX76, Program for Crystal Structure Refinement. University of Cambridge, U.K., 1974.

(16) *International Tables for X-ray Crystallography*; Kynoch Press: Birmingham, U.K., 1974; Vol. IV.

(17) Brodovitch, J.-C.; McAuley, A. *Inorg. Chem.* **1981**, *20*, 1667.

(18) Gore, E. S.; Busch, D. H. *Inorg. Chem.* **1973**, *12*, 1.

(19) Barefield, E. K.; Chueng, D.; Van Derveer, D. G. *J. Chem. Soc., Chem. Commun.* **1981**, 302.

Table II. Fractional Atomic Coordinates and Temperature Parameters[a]

atom	*x/a*	*y/b*	*z/c*	U_{eq}, Å
Ni(1)	20137 (18)	26854 (12)	-28659 (18)	302 (7)
Cl(1)	48223 (38)	34320 (26)	56042 (42)	443 (17)
Cl(2)	-1538 (47)	18381 (27)	-4783 (44)	518 (19)
O(1)	6021 (14)	3776 (9)	5254 (16)	97 (8)
O(2)	5110 (15)	2357 (9)	5514 (18)	107 (8)
O(3)	3132 (13)	3659 (10)	4380 (19)	124 (9)
O(4)	4943 (23)	3958 (13)	7330 (17)	155 (12)
O(5)	-1596 (12)	1337 (7)	-811 (12)	70 (6)
O(6)	3 (13)	1765 (8)	-2090 (12)	82 (6)
O(7)	-362 (20)	2895 (8)	366 (18)	124 (10)
O(8)	1396 (16)	1359 (13)	682 (18)	136 (10)
N(1)	236 (11)	3779 (7)	-3489 (10)	27 (4)
N(2)	3002 (11)	3440 (7)	-501 (11)	32 (4)
N(3)	3965 (11)	1601 (7)	-2178 (11)	35 (4)
N(4)	970 (11)	1969 (7)	-5391 (11)	36 (4)
C(1)	-415 (14)	4534 (8)	-2482 (14)	31 (6)
C(2)	455 (13)	4677 (8)	-518 (13)	28 (5)
C(3)	2260 (15)	4207 (9)	376 (14)	36 (6)
C(4)	4830 (14)	3014 (10)	502 (15)	45 (6)
C(5)	4819 (16)	1804 (9)	-155 (16)	47 (6)
C(6)	3647 (16)	471 (10)	-2958 (17)	51 (7)
C(7)	2818 (16)	250 (9)	-5025 (16)	49 (6)
C(8)	957 (16)	807 (9)	-5832 (16)	48 (6)
C(9)	-869 (14)	2492 (9)	-6225 (14)	38 (6)
C(10)	-735 (16)	3678 (9)	-5527 (14)	41 (6)

[a] Estimated standard deviations are given in parentheses. Coordinates are $\times 10^n$ where n = 5, 5, 4, 4, 4 for Ni, Cl, O, N, C. Temperature parameters are $\times 10^n$ where n = 4, 4, 3, 3, 3 for Ni, Cl, O, N, C. U_{eq} (equivalent isotropic temperature parameter) = $^1/_3 S_i S_j U_{ij} a_i^* a_j^* (a_i \cdot a_j)$.

Table III. Selected Interatomic Distances (Å) and Angles (deg)[a]

atoms	dist	atoms	angle
N(1)-Ni(1)	1.849 (9)	N(2)-Ni(1)-N(1)	91.5 (4)
N(2)-Ni(1)	1.851 (8)	N(3)-Ni(1)-N(1)	176.6 (4)
N(3)-Ni(1)	1.926 (8)	N(3)-Ni(1)-N(2)	86.8 (4)
N(4)-Ni(1)	1.940 (8)	N(4)-Ni(1)-N(1)	86.2 (4)
C(1)-N(1)	1.303 (12)	N(4)-Ni(1)-N(2)	176.6 (4)
C(3)-N(2)	1.290 (13)	N(4)-Ni(1)-N(3)	95.4 (4)
C(2)-C(2')	1.402 (20)	C(3)-C(2)-C(1)	121.6 (9)
C(1)-C(2)	1.459 (14)		
C(2)-C(3)	1.459 (15)		

[a] Estimated standard deviations are given in parentheses.

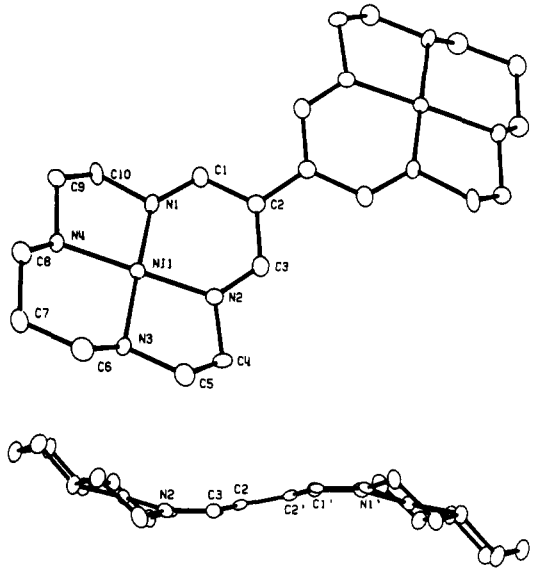

1a

1b

Figure 1. (a) ORTEP diagram of the $[Ni_2(L4)]^{4+}$ ion with 25% thermal ellipsoids. (b) Planar view of the molecular ion.

Ni(II) is coordinated in a square planar geometry by four nitrogens in each macrocycle (Table IV, plane 1) with a very weak interaction from an oxygen atom in one of perchlorate groups (at a distance of 2.734 Å). The average bond distance between Ni and imine nitrogens, d_{av}(Ni–N_{im}), is 1.850 (9) Å. Not only is this shorter than that (1.933 (8) Å) between Ni(II) and secondary amine nitrogens,[20] but also it is at the lower end of all Ni–N_{im} bonds (in *neutral* six-membered diimine rings) so far documented. Exceptionally short Fe–N_{im} lengths have also been reported for this ligand system.[14]

Table IV. Atomic Mean Planes

Plane 1

Equation: $(0.8464)X + (0.4817)Y + (-0.2273)Z - (5.5037) = 0$

atom	*X*	*Y*	*Y*	*P*	esd(*P*)	*P*/esd(*P*)
Ni(1)	3.6680	3.9725	-2.1171	-0.0047	0.0117	2.773
N(1)	2.7319	5.4991	-2.5771	0.0430	0.0098	4.369
N(2)	3.8562	4.5553	-0.3701	0.0383	0.0101	3.786
N(3)	4.7308	2.4480	-1.6092	0.0451	0.0101	4.463
N(4)	3.5054	3.4668	-3.9828	0.0382	0.0104	3.692
sum of *P*(I)				0.1600		

Plane 2

Equation: $(-0.5742)X + (-0.8171)Y + (-0.0514)Z - (-6.2253) = 0$

atom	*X*	*Y*	*Z*	*P*	esd(*P*)	*P*/esd(*P*)
C(1)	2.0033	6.3099	-1.8338	-0.0037	0.0117	0.314
C(2)	2.0783	6.1657	-0.3827	0.0137	0.0111	1.233
C(3)	3.1329	5.4048	0.2776	-0.0041	0.0124	0.334
C(2')	1.1115	6.8306	0.3827	-0.0137	0.0111	1.233
C(1')	1.1565	6.6864	1.8338	0.0037	0.0117	0.314
C(3')	0.0569	7.5915	-0.2776	0.0041	0.0124	0.334
sum of *P*(I)				0.0000		

Plane 3a

Equation: $(-0.8270)X + (-0.5572)Y + (-0.0740)Z - (-5.0909) = 0$

atom	*X*	*Y*	*Z*	*P*	esd(*P*)	*P*/esd(*P*)
Ni(1)	3.6680	3.9725	-2.1171	-0.0047	0.0117	0.214
N(1)	2.7319	5.4991	-2.5771	0.0430	0.0098	4.279
C(1)	2.0333	6.3099	-1.8338	0.0288	0.0125	2.306
C(10)	2.6435	5.7109	-4.0827	0.0244	0.0140	1.745
sum of *P*(I)				0.0115		

Plane 3b

Equation: $(0.6457)X + (0.7074)Y + (-0.2876)Z - (5.7875) = 0$

atom	*X*	*Y*	*Z*	*P*	esd(*P*)	*P*/esd(*P*)
Ni(1)	3.6680	3.9725	-2.1171	-0.0002	0.0016	0.145
N(2)	3.8562	4.5553	-0.3701	0.0312	0.0098	3.178
C(3)	3.1329	5.4048	0.2776	-0.0213	0.0125	1.702
C(4)	4.9037	3.8325	0.3711	-0.0169	0.0130	1.294
sum of *P*(I)				-0.0072		

As shown in Table III, and supplementary data, the angles around the three carbons in the diimine ring are all close to 120°, in agreement with in-plane sp^2 hybridization at these carbon centers. While sums of the bond angles around N(1) and N(2) are 359.5 and 359.7°, respectively, the C(1)–N(1)–Ni (130.0°) and C(3)–N(2)–Ni (128.6°) angles are much expanded from 120° and accompanied by a similar decrease in the C(10)–N(1)–Ni (113°) and C(4)–N(2)–Ni (113.1°) angles. Around Ni(II), the angles sum to 359.9°, consistent with the fact that the Ni atom is placed almost perfectly in the N_4 plane. However, the 91.5° N(1)–Ni–N(2) angle is somewhat larger than expected when the relatively short C(1)–C(2) and C(2)–C(3) bonds and the small N(1)–N(2) "bite", 2.651 Å, are considered.

As a whole, the molecule may be regarded as a series of planes which bend slightly (but do not *twist*) from one another. Figure 1b shows an ORTEP drawing of this molecule at an angle of 90° to that in Figure 1a. The molecule bends to maintain its center of symmetry and in the end gives an "S" shape. In this view, the two N_4 planes are parallel to each other.

(20) McAuley, A.; Subramanian, S.; Whitcombe, T. W. *J. Chem. Soc., Dalton Trans.* **1991**, 1821.

Table V. Comparison of Distances (Å) within the Six-Membered Imine Rings in Localized and Delocalized Systems

	$[Ni(AT)]^{+}$ [18]	$[Ni(ATH)]_2^{4+}$ [20]	$[Ni_2(L4)]^{4+}$	$[Fe_2(L_4)(CH_3CN)_2]^{4+}$ [14]
d_{av}(Ni—N_{imine})	1.83	1.887	1.850	1.89 (Fe–N)
d_{av}(C=N)	1.34	1.271	1.297	1.285
d_{av}(C—C)	1.40	1.501	1.459	1.45

In the center plane (Table IV, plane 2), the six carbons are all almost perfectly coplanar (estimated standard deviations are less than 0.012 Å), as expected from sp^2 hybridization at C(2) and C(2′). Similarly, the four nitrogens show very little, if any, tetrahedral deviation from their mean plane (1) (displacement of 0.003 Å), which is somewhat unusual when compared to many square planar tetraazamacrocyclic Ni(II) complexes which have some degree of tetrahedral distortion.[21] Confirmation of the planarity of the nitrogen donors of the diimine rings is provided (Table IV, planes 3a and 3b) where the adjoining atoms (e.g., C(10), C(1), Ni(1) around N(1)) are coplanar, consistent with an sp^2-hybridized center.

It is very interesting to compare the structure of the present molecule with that of $[Ni(AT)]^{+}$ [5] (**1**) and $[Ni^{II}_2(1,1'$-bi(2,13-dimethyl-3,6,9,12-tetraazacyclotrideca-2,12-dienylidene))], $[Ni(ATH)]_2^{4+}$ [12] (**5**). The common feature among these three molecules is that they all have a six-membered ring which contains six p_z orbitals (from Ni, two N_{im}'s, and three carbons). For this ring, the structural features in the present complex fall between those of the other two, which represent extremes of delocalized (in $[Ni(AT)]^{+}$) and localized (in $[Ni(ATH)]_2^{4+}$) diimine rings (Table IV).

In addition, while the ring in $[Ni(AT)]^{+}$ was found to be almost perfectly planar, the corresponding ring in the present compound is in a "boat" shape with an angle of about 150° between plane 1 and plane 2. Although the accurate shape of the sp^2 ring in $[Ni(ATH)]_2^{4+}$ [12] is not reported, from the displacement of 0.55 Å of the β-carbon out of the C=N plane, it is reasonable to estimate that the angle between the plane of Ni and the two imine nitrogens and that of the three carbons is less than 150°, with the ring more severely bent in the present case.

Formation of $[Ni^{II}_2(L4)]^{4+}$. After H_2O_2 was added at approximately 60 °C, the solution of $[Ni^{II}cyclam]^{2+}$ turned green (formation of Ni(III)), which persisted and then underwent a sudden change to deep purple. The resulting solution was not stable and converted to a brownish-yellow color (with decomposition) if kept at high temperature for more than 1 min.

The dimeric product is formed only in acidic media where $[H^+] > 0.2$ M ($X^{n-} = SO_4^{2-}$, NO_3^-, ClO_4^-). Also, formation occurred only at temperatures above 50 °C (the best yields obtained at 60–70 °C); otherwise only Ni(III) was produced. Sodium peroxodisulfate was the only other oxidant capable of oxidizing $[Ni^{II}cyclam]^{2+}$ to generate the dimer. Such observations are consistent with a radical mechanism. The effect of the metal center on the dimerization was also investigated by replacing Ni(II) with Cu(II). No similar reaction of $[Cu^{II}cyclam]^{2+}$ was observed.

Attempts were also made to isolate the reaction intermediates by analyzing either the final reaction mixture or the solution obtained prior to the deep-purple coloration. In both cases, the only species which were isolated and characterized were either the starting material or the dimer product (sometimes also $[Ni^{III}$-cyclam$]^{3+}$ in HNO_3 media).

Under the temperature conditions used, the Ni(III) formed is known to oxidize the solvent. Thus an equilibrium will be established involving Ni(II) and Ni(III) species. Oxidation of the Ni(II) complex by H_2O_2 provides a route to the transient Ni^{III}(hydroxo) ion and the hydroxyl radical. The latter is involved in the H atom abstraction at the ring nitrogen, and a subsequent intramolecular redox within the complex results in the formation of Ni(II) and OH•. In this regard, the chemistry is analogous

Scheme I

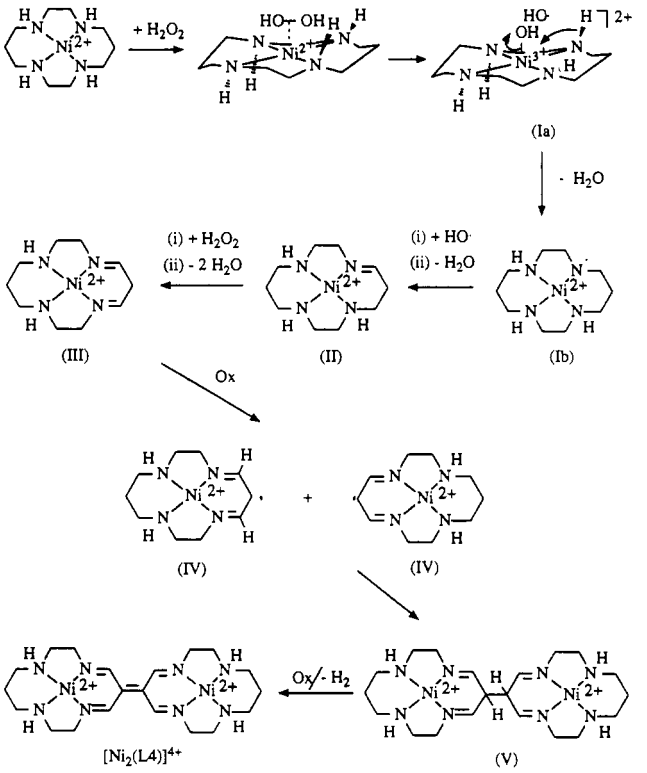

to that of Fenton's reagent in the reaction of Fe(II) systems with H_2O_2. The imine is formed by a second H atom abstraction. This process is repeated to form the diimine (II) (Scheme I). This proposed radical mechanism is also supported by the pulse-radiolysis study of the HO• radical oxidation of Ni(II) complexes of methyl-substituted tetraazamacrocyclic ligands where HO• attack on secondary amine and α-carbon hydrogens of the six-membered chelate ring were suggested to account for the formation of the imine group.[22] Further oxidation results in the formation of the Ni(II) radical cation (IV) which dimerizes (V) and is transformed readily to the final product. Although the final step shown in the reaction scheme is the formation of 1 mol of hydrogen, under the experimental conditions this was not observed. The release of protons could also account for the final oxidation product. To our knowledge the diene (II) is not known, probably owing to the facile deprotonation and coupling. An internal redox reaction has been postulated in the case of a Co(III)–dieno(–) complex, where cobalt(III) oxidizes the anion chelate to give a cobalt(II) ligand radical complex which subsequently dimerizes to the C–C bridged bicyclo product.[7,8]

Acidic conditions are required for the dimerization since hydrogen peroxide is a pH-dependent oxidant[23] ($E°$ = 1.77 V vs NHE). That dimerization occurred only after the green Ni(III) species was formed may explain why the dehydrogenation was inhibited by replacing Ni(II) with Cu(II), where there is a higher $E°$ for the $Cu^{II}/^{III}$ couple. The crystallographic structure of $[Ni^{III}$-cyclam$(NO_3)](NO_3)$ has been resolved recently[24] and showed cyclam to be in a *trans*-III conformation with the two secondary

(21) Curtis, N. F. Reference 1, p 219.

(22) Whitburn, K. D.; Laurence, G. S. *J. Chem. Soc., Dalton Trans.* **1979**, 139.

(23) Sharpe, A. G. *Inorganic Chemistry*, 2nd ed.; Longman Inc.: New York, 1986; p 384.

(24) McAuley, A.; Palmer, T. A. Unpublished results.

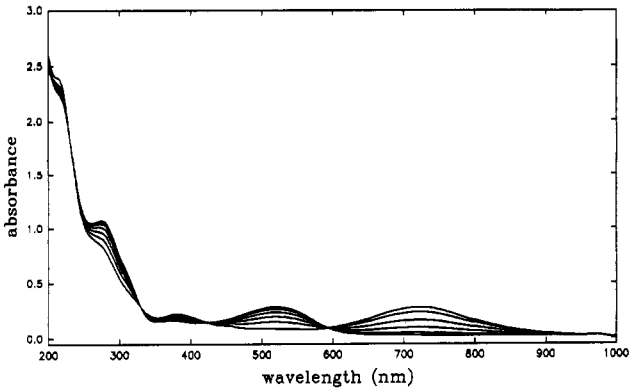

Figure 2. UV/visible spectra of the $[Ni_2(L4)]^{4+}$ ion (λ_{max} 520 nm) and the related radical cation (λ_{max} 724 nm). The traces show the spectra resulting from the aerial oxidation of the radical species with isosbestic points at 229, 330, 424, and 593 nm respectively.

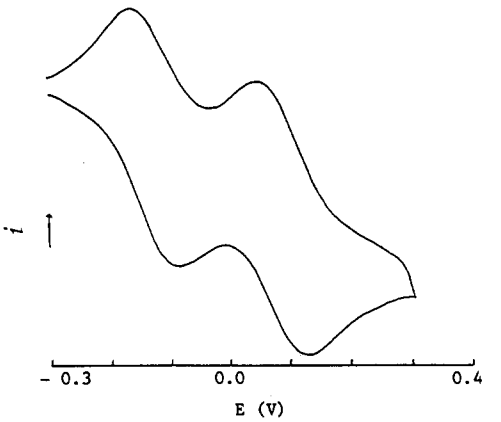

Figure 3. Cyclic voltammetry of the reduction of the $[Ni_2(L4)]^{4+}$ ion in acetonitrile showing the two-step process with the radical ion VI as intermediate.

amines of the six-membered ring cis to each other. This configuration would permit dehydrogenation in the ring.

UV/Visible Spectra and Solution Chemistry. In aqueous acidic media, the electronic spectrum of the $[Ni_2(L4)]^{4+}$ dimer species is characterized by an intense absorption band in the visible region (λ_{max} 520 nm, $\epsilon = 6.5 \times 10^3$ M^{-1} cm^{-1}) (Figure 2) and two UV bands, at 277 nm ($\epsilon = 1.5 \times 10^4$ M^{-1} cm^{-1}) and 200 nm ($\epsilon = 1.7 \times 10^4$ M^{-1} cm^{-1}). The wavelength maximum, λ_{max}, of the visible band was dependent upon the counterion. In the presence of NO_3^-, SO_4^{2-}, and F^-, the visible spectrum is little different from that in water. However, on a change from F^- to I^-, λ_{max} showed a progressive "red shift" from 528 to 547 nm. This indicates the presence of an axial coordination on Ni(II) centers with these halides (and SCN^-). A strong charge-transfer band has been observed for the analogous Fe(II) complex with comparable effects of axial ligation.[14]

The bicyclic ion is not stable in neutral aqueous solution and converts slowly ($t_{1/2} \sim 25$ min) to a yellow species (shoulder at λ_{max} 380 nm). The isosbestic point observed at λ 405 nm is consistent with no intermediate or decomposition involved. Addition of perchloric acid shortly after the purple coloration disappeared provided evidence for reversibility of the process with about 100% recovery of starting material. However, when the yellow solution formed was left to stand for long periods, only partial recovery of the initial dimer species was possible.[25] The spectrum of the yellow ion is inconsistent with the formation of any octahedral nickel(II) ions, and a possible explanation lies in the addition of 1 mol of water across the double bond, which upon further deprotonation leads to the formation of a dieno(–) species. Substantiation of this conclusion must await NMR data on the reaction.

Electrochemical Studies. Oxidation in aqueous media (pH 3) showed only a weak anodic shoulder peak at about 1.18 V vs NHE (oxidation at the metal center) with no cathodic wave present. In CH_3CN, a quasi-reversible wave was seen at $E'_{1/2}$ = 1.06 V (1.46 V vs NHE). The redox peaks were sensitive to scan rate even at <20 mV/s. Of interest is that in acetonitrile only one redox peak was observed in the range 0.5–1.4 V. For a molecule with two reactive centers, if both electron-transfer processes are reversible, ΔE should be 35.6 mV. The appearance of only one wave may result from coupled electron transfers between interacting reaction centers.

Reduction of the conjugated dimer complex gave rise to two reversible couples in both CH_3CN (Figure 3) and aqueous acidic media (pH <3). A reaction scheme accounting for the electron-transfer processes is presented in Scheme II. In aqueous acidic nitrate media, the potential for the first reduction ($E_{1/2}^1$ = 0.40 V vs NHE) is independent of counterion, consistent with the

Scheme II

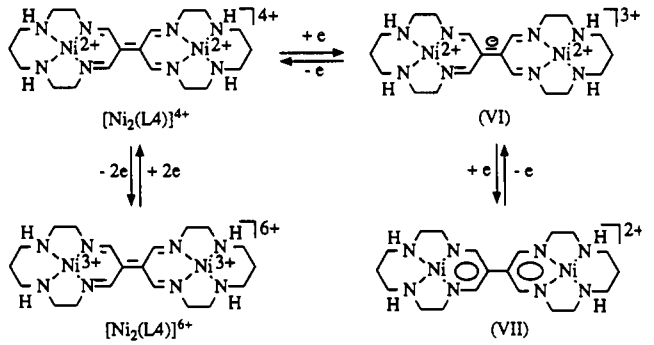

formation of a 1-e-reduced species (VI), where the electron was delocalized on the π_M orbital. A second wave was observed at 0.21 V vs NHE.

In CH_3CN, redox couples were exhibited at $E_{1/2}^1$ = 0.19 V and $E_{1/2}^2$ = –0.03 V vs $Fc^{+/0}$ (0.60 and 0.37 V vs NHE). The higher potential indicates that the unsaturated dimer may be regarded as a moderate oxidizing agent (indeed, it can oxidize I^- readily in CH_3CN). No further reduction was observed to –1.4 V, consistent with the stable two-"aromatic"-ring structure of VII.

Confirmation of the formation of a green Ni(III) ion in the electrochemical study was provided by reaction of the Ni(II) dimer with Co_{aq}^{3+} or $Na_2S_2O_8$ in acidic aqueous media and NO^+ in acetonitrile. The ESR spectrum of the product obtained in both solvents was characteristic of a tetragonally-elongated low-spin Ni(III) (indicating that the oxidation was metal-based) without the appearance of a metal–metal interaction. In CH_3CN, the spectrum showed five shf-coupling peaks ($A_\parallel$ = 20 G) from two axially-coordinated solvent molecules ($g_\parallel$ = 2.025, $g_\perp$ = 2.177) virtually identical to those of $[Ni^{III}cyclam]^{3+}$ [18] under the same conditions (Figure 4a). The ESR spectrum obtained from oxidation in 1.0 M nitric acid also showed axial symmetry, with $g_\parallel$ = 2.022 and $g_\perp$ = 2.287. In both solvents, the oxidized species were of limited stability (t < 1 min).

Chemical reduction of the unsaturated dimer, characterized by a deep-green coloration (Figure 2), was achieved using ascorbic acid, Zn dust, Fe^{2+}, and $[Co(phen)_3]^{2+}$ in aqueous media or ferrocene and I^- ($(t\text{-}Bu)_4N^+$ salt) in CH_3CN. In both solvents, the reduction product (VI) exhibits a pronounced band at λ 724 nm ($\epsilon = 1.3 \times 10^4$ M^{-1} cm^{-1}, significantly greater than for the purple $[Ni_2(L4)]^{4+}$ species). In aqueous media, there is also a weak band at 382 nm and a pronounced shoulder at 217 nm. The species is stable in aqueous media under argon but reacts readily upon opening to air. A UV/visible study of the aerial oxidation showed four isosbestic points in the transformation to the purple dimer (Figure 2), reflecting the reversible nature of the process.

(25) Xu, C. Ph.D. Dissertation, University of Victoria, 1991.

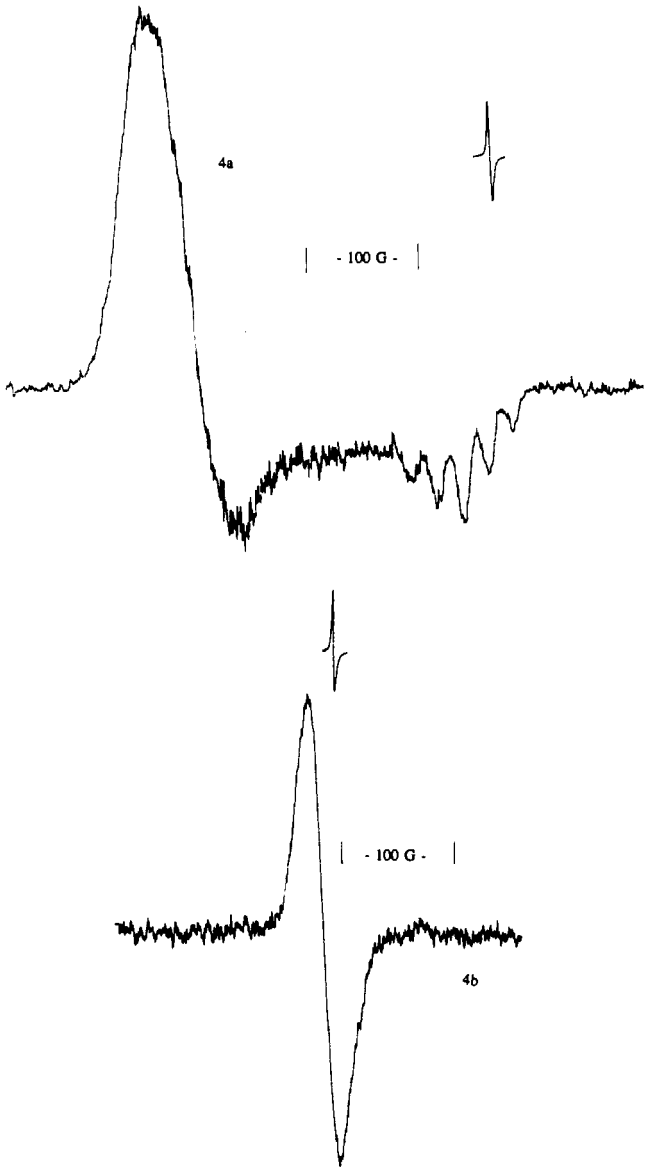

Figure 4. ESR spectra recorded at 77 K: (a) $[Ni^{III}_2(L4)]^{6+}$ formed by oxidation of the dinuclear Ni(II) species by NO^+ in acetonitrile; (b) radical ion VI in CH_3CN.

ESR spectra of the reduction product in both water and acetonitrile showed a symmetric peak at $g = 2.007$ (peak width ~ 25 G) (Figure 4b), which is greater than that normally observed for organic radicals. Variations of solvent, supporting electrolyte, and temperature failed to produce any nitrogen-coupled ESR spectrum. Similarly, no metal coupling was observed when ^{61}Ni was used. In this regard, the formulation of the ion must take into account a delocalization of the electron across the two metal centers with some Ni(I) character involved. Of interest is a comparison of the ESR spectrum of radical VI with that of the reduction product of tetracyanoethylene, $[TCNE^{\bullet}]^-$, where a high degree of electron density delocalization to the conjugated molecular plane has been demonstrated.[26-28] The g value observed, 2.0036,[26] is lower than the found in the present study (2.007), and the fact that extensive fine structure is identified in the organic free radical and not in VI probably reflects the influence of the metal orbital component in the overall delocalized dinuclear π-system. No extensive investigation of the product of the second reduction was carried out.

Kinetic Studies. A preliminary kinetic study of the reduction of the conjugated bicyclic complex was performed at 9 °C using $[Co(phen)_3]^{2+}$ as reductant in 1.0 M $H/NaNO_3$. Under the conditions of a large excess of the reducant, k_{obs}, the pseudo-first-order rate constant (monitoring at 520 nm), showed a linear dependence on [reductant] ($k_{obs} = k_1[Co(II)]$) where $k_1 = 7.8 \times 10^4$ M^{-1} s^{-1}. The experimental data are presented in the supplementary material. The simplified Marcus cross-relation[29] was used to calculate a self-exchange rate constant for the $[Ni_2(L4)]^{4+/3+}$ couple, $k_{11} = 5.1 \times 10^6$ M^{-1} s^{-1} (9 °C).

In the kinetic experiments, it was observed that when the reaction was monitored at 720 nm, the reaction traces were biphasic. By monitoring the reaction at the isosbestic point (593 nm) of the first step, we could observe the second redox reaction. In this case, a nonlinear dependence on the reductant concentration was observed, which is the subject of further investigation.

Both structural features and chemical reactivities of $[Ni^{II}_2(L4)]^{4+}$ may be best described by its delocalized electron density over a largely unsaturated and conjugated system. With respect to redox chemistry, TCNE may serve as a model for the π delocalization in present case. The reduction potential of TCNE is 0.152 V vs SCE in acetonitrile[26] (0.39 V vs NHE). This is somewhat lower than that (0.6 V vs NHE) of the dimer complex. However, the reduction potential of $[TCNE^{\bullet}]^-$ is reported to be −0.32 V vs NHE, condiserably lower than 0.37 V vs NHE for the metal-based radical anion.

The rate of self-exchange for the first 1-e reduction, 5.1×10^6 M^{-1} s^{-1}, is 40 times smaller than that, 2.1×10^8 M^{-1} s^{-1}, in the case of TCNE.[27] The extent of this decrease in rate may reflect some bond rearrangement within the dinuclear complex ion, but when compared with values for other Ni(II/III) couples (10^3–10^4 M^{-1} s^{-1} [30]) the higher value is consistent with electron delocalization reducing the intrinsic reorganizational barrier to electron transfer. However, these values must be viewed as preliminary, since reorganizational effects on the rate of electron transfer may be strongly solvent dependent. Further work in this area is under consideration.

Acknowledgment. We thank the Natural Sciences and Engineering Research Council (Canada) for support and the University of Victoria for a fellowship award to C.X. The assistance of Kathy Beveridge in the X-ray determination is gratefully acknowledged.

Supplementary Material Available: Tables S1–S5, containing experimental crystallographic data, anisotropic temperature parameters, bond lengths and bond angles, and intermolecular distances, and Table S6, listing kinetic data for the reduction of the complex with $[Co(phen)_3]^{2+}$ (8 pages). Ordering information is given on any current masthead page.

(26) Webster, O. W.; Mahler, W.; Benson, R. E. *J. Am. Chem. Soc.* **1962**, *84*, 2210.
(27) Phillips, W. D.; Rowell, J. C. *J. Chem. Phys.* **1960**, *33*, 626.
(28) Webster, O. W.; Mahler, W.; Benson, R. E. *J. Org. Chem.* **1960**, *25*, 1470.
(29) Marcus, R. A. *Annu. Rev. Phys. Chem.* **1964**, *15*, 155; *J. Chem. Phys.* **1965**, *43*, 679.
(30) McAuley, A.; Macartney, D. H.; Oswald, T. *J. Chem. Soc., Chem. Commun.* **1982**, 274. McAuley, A.; Norman, P. R.; Olubuyide, O. *Inorg. Chem.* **1984**, *23*, 2953.